Eur J Nucl Med Mol Imaging (2012) 39:621–631
DOI 10.1007/s00259-011-2021-8

ORIGINAL ARTICLE

Using PET with ^{18}F-AV-45 (florbetapir) to quantify brain amyloid load in a clinical environment

V. Camus · P. Payoux · L. Barré · B. Desgranges · T. Voisin · C. Tauber · R. La Joie · M. Tafani · C. Hommet · G. Chételat · K. Mondon · V. de La Sayette · J. P. Cottier · E. Beaufils · M. J. Ribeiro · V. Gissot · E. Vierron · J. Vercouillie · B. Vellas · F. Eustache · D. Guilloteau

Received: 29 July 2011 / Accepted: 2 December 2011 / Published online: 18 January 2012

Abstract
Purpose Positron emission tomography (PET) imaging of brain amyloid load has been suggested as a core biomarker for Alzheimer's disease (AD). The aim of this study was to test the feasibility of using PET imaging with ^{18}F-AV-45 (florbetapir) in a routine clinical environment to differentiate between patients with mild to moderate AD and mild cognitive impairment (MCI) from normal healthy controls (HC).
Methods In this study, 46 subjects (20 men and 26 women, mean age of 69.0±7.6 years), including 13 with AD, 12 with MCI and 21 HC subjects, were enrolled from three academic memory clinics. PET images were acquired over a 10-min period 50 min after injection of florbetapir (mean ± SD of

V. Camus (✉) · C. Tauber · C. Hommet · K. Mondon · J. P. Cottier · E. Beaufils · M. J. Ribeiro · E. Vierron · J. Vercouillie · D. Guilloteau
UMR INSERM U930-CNRS ERL 3106,
Tours, France
e-mail: vincent.camus@univ-tours.fr

V. Camus · C. Tauber · C. Hommet · K. Mondon · J. P. Cottier · E. Beaufils · M. J. Ribeiro · E. Vierron · J. Vercouillie · D. Guilloteau
Université François Rabelais de Tours,
Tours, France

V. Gissot · D. Guilloteau
CIC-IT /CIC INSERM 202,
Tours, France

V. Camus · C. Tauber · C. Hommet · K. Mondon · J. P. Cottier · E. Beaufils · M. J. Ribeiro · V. Gissot · J. Vercouillie · D. Guilloteau
CHRU de Tours,
Tours, France

P. Payoux · M. Tafani
INSERM U825,
Toulouse, France

P. Payoux · T. Voisin · M. Tafani · B. Vellas
Université Paul Sabatier de Toulouse,
Toulouse, France

L. Barré
Groupe de Développements Méthodologiques en Tomographie par Émission de Positons, CEA/DSV/I2BM/CI-NAPS UMR6232,
Caen, France

L. Barré
Université de Caen Basse Normandie,
Caen, France

B. Desgranges · R. La Joie · G. Chételat · V. de La Sayette · F. Eustache
INSERM U1077,
Caen, France

B. Desgranges · R. La Joie · G. Chételat · V. de La Sayette · F. Eustache
Université de Caen Basse Normandie - UMR-S1077,
Caen, France

B. Desgranges · R. La Joie · G. Chételat · V. de La Sayette · F. Eustache
Ecole Pratique des Hautes Etudes, UMR-S1077,
Caen, France

T. Voisin · B. Vellas
INSERM U1027,
Toulouse, France

P. Payoux · T. Voisin · M. Tafani · B. Vellas
CHRU de Toulouse,
Toulouse, France

radioactivity injected, 259±57 MBq). PET images were assessed visually by two individuals blinded to any clinical information and quantitatively via the standard uptake value ratio (SUVr) in the specific regions of interest, which were defined in relation to the cerebellum as the reference region.

Results The mean values of SUVr were higher in AD patients (median 1.20, Q1-Q3 1.16-1.30) than in HC subjects (median 1.05, Q1-Q3 1.04-1.08; $p=0.0001$) in the overall cortex and all cortical regions (precuneus, anterior and posterior cingulate, and frontal median, temporal, parietal and occipital cortex). The MCI subjects also showed a higher uptake of florbetapir in the posterior cingulate cortex (median 1.06, Q1-Q3 0.97-1.28) compared with HC subjects (median 0.95, Q1-Q3 0.82-1.02; $p=0.03$). Qualitative visual assessment of the PET scans showed a sensitivity of 84.6% (95% CI 0.55–0.98) and a specificity of 38.1% (95% CI 0.18–0.62) for discriminating AD patients from HC subjects; however, the quantitative assessment of the global cortex SUVr showed a sensitivity of 92.3% and specificity of 90.5% with a cut-off value of 1.122 (area under the curve 0.894).

Conclusion These preliminary results suggest that PET with florbetapir is a safe and suitable biomarker for AD that can be used routinely in a clinical environment. However, the low specificity of the visual PET scan assessment could be improved by the use of specific training and automatic or semiautomatic quantification tools.

Keywords ^{18}F-AV-45 · Florbetapir · Alzheimer's disease · PET imaging · Brain imaging

Introduction

The use of positron emission tomography (PET) imaging with probes that bind specifically to β-amyloid and tau aggregates has received increased attention recently because this technique may provide an earlier diagnosis of Alzheimer's disease (AD). Currently, AD [1, 2] must reach the dementia stage, in which cognitive and noncognitive symptoms significantly alter activities of daily living, to be clinically diagnosed. However, disease symptoms are considered a consequence of the cumulative burden of brain alterations that may begin to appear years before initial clinical manifestations [3, 4]. Consequently, the new AD diagnostic criteria suggest that the diagnosis of "prodromal AD" (also called the AD predementia stage) [5] or "MCI due to AD pathology" [6] should rely on in-vivo biomarkers of amyloid pathology, such as PET imaging that uses ligands of amyloid plaques and degenerative neurofibrillary tangles. Among the candidate probes, ^{11}C-labelled tracers have been extensively studied. The PIB compound (*N*-methyl-[^{11}C]2-(4′-methylaminophenyl)-6-hydroxybenzothiazole), a derivative of thioflavin T, was the first to demonstrate the ability to clearly distinguish AD patients from healthy control (HC) subjects [7]. PET imaging with ^{11}C-PIB has also been used to efficiently differentiate patients with mild cognitive impairment (MCI) who have converted to AD from nonconverters [8], and to estimate the decreased amyloid load in patients treated with bapineuzumab [9]. Nevertheless, ^{11}C-PIB uptake is also increased in nondemented elderly subjects [10] and shows a variable level of agreement with other biomarkers, such as cerebrospinal fluid (CSF) dosage of Aβ [11]. Another ^{11}C-labelled, benzoxazole-derived compound, ^{11}C-BF-227, has good neocortical uptake in AD patients [12] and appears to be able to discriminate MCI converters from nonconverters better than voxel-based morphometry using magnetic resonance imaging (MRI) [13, 14]. However, the 20-min radioactive half-life of both ^{11}C-PIB and ^{11}C-BF-227 is a serious barrier to increasing the accessibility of biomarkers for routine clinical purposes, as the use of these markers is limited to centres with an on-site cyclotron.

Consequently, ^{18}F-labelled amyloid ligands appear to be the best alternative, as the 110-min half-life of ^{18}F allows the centralized production and locoregional delivery of compounds, similar to other PET radiotracers, such as ^{18}F-FDG. Several clinical studies have been conducted with a new naphthalene family compound, 2-(1-{6-[(2-^{18}F-fluoroethyl)(methyl)amino]-2-naphthyl}ethylidene)malononitrile (^{18}F-FDDNP). PET with ^{18}F-FDDNP has demonstrated the ability to discriminate between HC subjects, MCI patients and AD patients [15]. However, ^{18}F-FDDNP has limitations because of its low metabolic stability and its high white matter binding [16]. More recently, the standard uptake value ratio (SUVr) of ^{18}F-labelled PIB (^{18}F-flutemetamol) was observed to be highly correlated with the SUVr of its parent molecule, ^{11}C-PIB [17]. However, another family of ^{18}F-labelled ligands derived from stilbene has been developed, and two compounds belonging to this family (AV-1 and AV-45) display favourable properties for brain amyloid PET imaging. ^{18}F-AV1 (BAY-94-9172, florbetaben) has brain kinetic characteristics appropriate for clinical use. When studied 90 to 120 min after injection, the level of cortical uptake clearly distinguished 15 AD patients from 15 healthy elderly subjects [18]. A recent phase II study has shown that the visual rating of PET scans with florbetaben has sufficient sensitivity (80%) and specificity (91%) to distinguish AD patients from HC subjects [19].

The last stilbene family derivative, ^{18}F-AV-45 (florbetapir) [20], also has strong affinity for amyloid proteins in AD brain homogenates (*k*i 10±3.3 nM) and faster in vivo kinetics [21]. The use of florbetapir in amyloid imaging has recently been validated in an autopsy study [22], and its safety profile allows clinical applications in brain imaging [23]. A pilot study comparing 16 AD patients with 16 HC subjects confirmed that florbetapir binds selectively to amyloid proteins enabling AD patients to be distinguished from HC subjects, and has kinetics that allow imaging sessions as short as 10 min 50 to 60 min or 60 to 70 min after injection [24]. More recently, a multicentre

study conducted at 31 US research sites that included 82 elderly HC subjects, 62 AD patients and 62 MCI patients reported that both qualitative visual ratings and a continuous mean cortical SUVr quantification show high sensitivity and specificity for distinguishing AD patients from MCI patients and elderly HC subjects [25]. These findings suggest that florbetapir is a useful biomarker for distinguishing AD and MCI patients from HC subjects. However, these results were derived from premarketing studies, and little is known about their possible replication under "real life" conditions and everyday practice.

In the present study, our aim was to assess the feasibility of using PET imaging with florbetapir in third-level clinical settings to differentiate patients with mild to moderate AD or MCI patients from normal HC subjects in three PET centres. In addition, we assessed the safety of a florbetapir injection immediately after injection and during the follow-up period.

Methods

Subjects

Patients consecutively referred to the three participating memory clinics (from the university hospitals of Tours, Caen and Toulouse in France) and who met the NINCDS-ADRDA criteria for probable AD and DSM-IV criteria for Alzheimer's type dementia or diagnostic criteria for amnestic MCI [26, 27] were allowed to participate. All participants had to be at least 55 years of age, able to speak French fluently, have completed at least 7 years of education and have neither unstable somatic disease nor psychiatric comorbidities. HC subjects were recruited through a community advertisement and investigated in the same clinical settings. AD patients were required to have a mini-mental state examination (MMSE) score between 15 and 28. The diagnosis was made considering the guidelines for global neuropsychological testing [28] and an evaluation of verbal episodic memory (Free and Cued Selective Reminding Test, FCSRT) [29], language (verbal fluency, naming, comprehension) [30], gnosis [31], praxis [32], visuospatial functions [33] and executive functions [34–36]. AD patients were excluded if they had any past or current symptomatic treatment with acetylcholinesterase inhibitors or memantine or had participated in any experimental study investigating A-β-lowering agents. MCI patients were required to have a subjective memory complaint associated with isolated impairment in episodic memory, assessed by a free recall total score (based on the FCSRT) of less than 1.5 SD from the means for their age and education level. Healthy controls could not have any past history of or current major depressive episodes and/or antidepressant treatment, cognitive impairment in the diagnostic neuropsychological battery, memory complaints, or MRI brain scan abnormalities.

Vital signs and clinical status were checked before and after scanning, and follow-up visits were systematically conducted 1 year after inclusion. Adverse events and serious adverse events were assessed from the first administration of the tracer, immediately after the scan and during the follow-up period.

According to French regulations and laws on biomedical research, the study was approved by the ethics committee of Tours (*Comité de Protection des Personnes de la Région Centre*) and the French Agency for Safety and Security for Medical Devices (*Agence Française de Sécurité Sanitaire des Produits de Santé,* reference A81216-27). The study was also registred in the ClinTrials database under N° NCT01325259. Written informed consent was obtained from all patients and HC subjects who entered the study and from the next of kin of all participating patients. All participants were asked to sign a specific consent form for ApoE genotyping, according to French regulations. The ethics committee approved the consent procedure.

A total of 46 subjects (20 men, 26 women, mean age 69.0± 7.6 years) were included in the study, including 13 AD patients, 12 MCI patients and 21 HC subjects. The demographic and clinical characteristics of the 46 subjects are presented in Table 1. ApoE genotyping was available for 38 subjects.

^{18}F-AV-45 (florbetapir) synthesis

Florbetapir) was prepared by the nucleophilic substitution of a tosylate precursor (*E*)-2-(2-(2-(5-(4-(*tert*-butoxycarbonyl (methyl)amino)styryl)pyridin-2-yloxy)ethoxy)ethoxy)ethyl-4-methylbenzenesulphonate (AV-105) provided by Avid Radiopharmaceuticals (Philadelphia, PA) with a GMP certificate, on an automatic synthesizer according to previously described methods [37]. The radiochemical purity and specific activity were approximately 98% and 180±70 GBq/μmol (mean ± SD values of 20 experiments), respectively. The radiochemical yields were 40–45%.

Image acquisition

MRI A brain MRI scan was performed in all subjects using a 1.5-T imager in one centre (Tours), and 3-T imagers in the other two centres (Caen, Toulouse). T2-weighted images from each subject were used to investigate brain lesions.

PET Subjects were examined using whole-body hybrid PET/CT scanners, including a Dual Gemini (Philips Medical Systems), a Discovery RX VCT 64 (General Electric) and a Biograph 6 TruePoint HiRez (Siemens Medical Solutions) in Tours, Caen and Toulouse, respectively. All tomographs operated in 3-D detection mode. For the three centres, the acquisition data were processed by adapting the reconstruction parameters to those of the tomograph with the lowest spatial resolution (Dual Philips GEMINI) to ensure that the images could be matched. All PET sinograms were reconstructed with a 3-D iterative algorithm, with corrections for

Table 1 Demographic and clinical characteristics of subjects included in the PET study

Characteristic	AD patients	MCI patients	HC subjects	*p*-value			
				Global	AD vs. HC	AD vs. MCI	MCI vs. HC
Gender (male/female, *n*)	4/9	7/5	9/12	0.380	–	–	–
Age (years)							
n	13	12	21				
Median (Q1, Q3)	68.0 (65.0, 74.0)	72.5 (69.5, 81.8)	66.0 (63.0, 68.0)	0.023	–	–	–
Mean (SD)	67.8 (6.5)	75.0 (10.1)	66.2 (4.3)				
MMSE							
n	11	12	21				
Median (Q1, Q3)	23.0 (21.0, 25.0)	26.5 (24.5, 27.3)	29.0 (29.0, 30.0)	<0.0001	<0.0001	–	0.002
Mean (SD)	23.0 (3.6)	25.9 (2.9)	29.0 (1.3)				
MATTIS							
n	11	12	21				
Median (Q1, Q3)	126.0 (112.5, 129.5)	125.0 (119.3, 137.5)	143.0 (142.0, 144.0)	<0.0001	<0.0001	–	<0.0001
Mean (SD)	119.9 (14.6)	126.7 (11.0)	142.8 (1.4)				
FCRST immediate free recall							
n	11	12	21				
Median (Q1, Q3)	10.0 (6.5, 14.0)	15.0 (14.0, 16.0)	16.0 (16.0, 16.0)	<0.0001	<0.0001	0.010	0.010
Mean (SD)	10.0 (4.6)	14.3 (2.6)	15.7 (0.6)				
FCRST immediate free and cued recall							
n	10	12	21				
Median (Q1, Q3)	17.0 (16.0, 26.5)	30.0 (20.8, 36.3)	47.0 (46.0, 48.0)	<0.0001	<0.0001	–	<0.0001
Mean (SD)	21.2 (11.4)	27.4 (13.8)	46.2 (2.7)				
FCRST delayed free recall							
n	8	11	14				
Median (Q1, Q3)	2.5 (0.0, 9.5)	6.0 (0.5, 12.0)	13.0 (12.3, 14.0)	0.019	–	–	–
Mean (SD)	5.4 (6.7)	8.3 (9.3)	13.1 (1.9)				
FCRST delayed free and cued recall							
n	8	10	12				
Median (Q1, Q3)	9.5 (2.5, 11.3)	9.0 (3.3, 12.0)	16.0 (16.0, 16.0)	0.002	0.004	–	0.003
Mean (SD)	7.8 (5.8)	7.9 (6.0)	14.7 (4.6)				
ApoE genotype							
n	10	9	19				
ε4 carrier, *n* (%)	7 (70)	6 (67)	8 (42)	0.332	–	–	–
ε4 non carrier, *n* (%)	3 (30)	3 (33)	11 (58)				

randomness, scatter, photon attenuation and decay, which produced images with an isotropic voxel of 2×2×2 mm and a spatial resolution of approximately 5-mm full-width at a half-maximum at the field of view centre. The acquisition data were processed using the standard package provided with each acquisition system. All cerebral emission scans began 50 min after a mean injection of 4 MBq/kg weight of florbetapir (mean ± SD injected radioactivity 259± 57 MBq). For each subject, two 10-min frames were acquired to ensure movement-free image acquisition, but only the first frame was qualitatively and quantitatively analysed.

Image analysis

The florbetapir PET images were coregistered to the florbetapir template proposed by Wong et al. [24] in the Talairach space using PMOD v3.1 (PMOD Technologies) with a mutual information similarity function. Standardized uptake values (SUVs) were obtained by normalizing the tissue concentration to the injected dose and body weight. The regional-to-cerebellum SUVr was used for intersubject comparison [38] because the cerebellum has been reported to be a region free of fibrillar amyloid plaques in AD brains [36]. Each regional SUVr value was expressed as the mean over

the region of interest (ROI) and as the mean of the left and right corresponding regions. To define the ROIs for analysis, the grey and white matter, CSF and skull were identified in the MR images of ten healthy subjects. ROIs were created in the following 13 regions: precuneus, anterior cingulate, posterior cingulate, frontal, temporal, parietal, occipital, hippocampus, centrum semiovale, anterior putamen, posterior putamen, caudate nucleus and pons.

Florbetapir PET images were also visually assessed by two independent raters, who were nuclear medicine specialists and blinded to all clinical and diagnostic information. The raters used a binary scale to classify each scan as 0 (no significant florbetapir cortical uptake) and 1 (significant florbetapir cortical uptake). Prior to this assessment, the raters underwent a half-day training session on a training set provided by AVID pharmaceuticals. The visual rating was re-run by the two raters until they reached full agreement for each discrepant case.

Statistical analysis

Descriptive statistics and tests were separately computed for the AD, MCI and control subjects. The chi-squared test and Fisher's exact test were applied to assess differences in gender or in ApoE ε4 genotype between groups and visual rating categories. To compare the distributions of the continuous

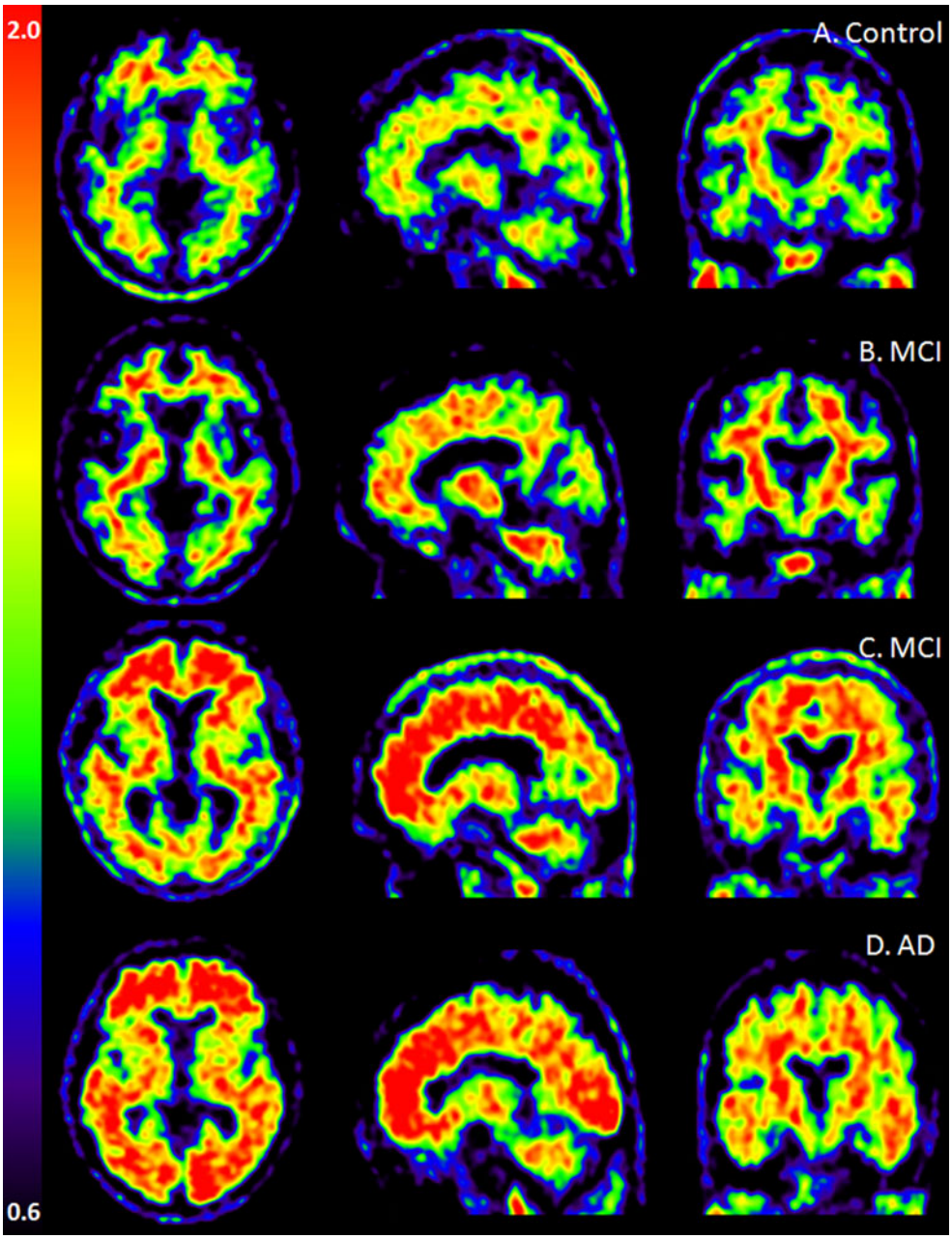

Fig. 1 Representative axial, sagittal and coronal florbetapir-negative images of a HC subject (**a**) and a MCI patient (**b**), and florbetapir-positive images of a MCI patient (**c**) and an AD patient (**d**)

variables between groups, including SUVr, the Kruskal-Wallis rank sum test was used. When significant global *p*-values were obtained, pair-wise comparisons between the three groups were performed using the Wilcoxon rank sum test, and *p*-values were adjusted for multiple comparisons using the false discovery rate method. All tests were two-sided. Mann-Whitney tests were performed to compare the SUVr between the two ApoE statuses in each group. The significance level was set at $p<0.05$. The sensitivity and specificity of the visual rating (PET-positive vs. PET-negative) were determined using the clinical diagnosis as the gold standard. Inter-rater agreement of the visual assessments was estimated by calculating Cohen's kappa (κ) and its 95% confidence interval (95% CI). A ROC curve analysis allowed us to study the diagnostic power of the cortex global ROI SUVr against clinical diagnoses, and the area under the curve was calculated. The sensitivity and specificity were also calculated at the optimal cut-off point. Statistical analyses were performed using R software version 2.12.2 [38].

Results

Overall, the PET scan procedures were well tolerated, and no serious adverse events were reported during the immediate follow-up period. At the 1-year follow-up, one patient had bladder cancer, and another was hospitalized for a ruptured aortic aneurysm. Both were considered serious adverse events without evidence of a causal relationship with the protocol procedures.

Visual analysis

Agreement analysis between the two raters yielded a κ value of 0.71 (95% CI 0.50–0.93), which indicates substantial agreement. Compared with the initial clinical diagnosis, the visual PET scan rating classified 11 of the 13 AD patients (85%) and 13 of the 21 HC subjects (60%) as positive. A calculation of the visual sensitivity and specificity compared with the clinical diagnosis yielded values of 84.6% (95% CI 0.55–0.98) and 38.1% (95% CI 0.18–0.62), respectively. Among the MCI subjects, six were assigned to the positive category and six to the negative category. Axial, sagittal and coronal section slices of representative positive AD and MCI patient scans and negative MCI and HC patient scans are shown in Fig. 1. As shown in Table 2, being an ApoE genotype carrier and uptake in the global cortical ROI were the factors most significantly associated with a positive PET visual assessment.

Quantitative analysis

Descriptive statistics and tests of ROI-to-cerebellum SUVr for AD patients, MCI patients and HC subjects are presented in Table 3. The mean values of SUVr were significantly higher in AD patients than in HC subjects in the overall cortex and most cortical regions (i.e. the precuneus, anterior and posterior cingulate, temporal and frontal median regions) (Fig. 2). Moreover, significant differences were also observed between AD and MCI patients in the precuneus ($p=0.045$), posterior cingulate ($p=0.030$) and frontal median ($p=0.045$) regions. Significantly higher florbetapir uptake in the posterior cingulate region was also found in MCI patients than in HC subjects ($p=0.030$). The ROC curve analysis showed the best sensitivity (92.3%) and specificity (90.5%) values with a cut-off value of 1.122 (area under the curve 0.894). As shown in Table 4, florbetapir uptake among AD patients was significantly higher in ApoE carriers than in non-carriers in the precuneus, anterior cingulate, posterior cingulate, frontal median and temporal cortical regions, and among MCI patients in the anterior cingulate, posterior cingulate and frontal median cortical regions.

Table 2 Age, ApoE genotype, cortical ROI and FCRST free immediate recall scores according to visual rating

	Visual rating		*p*-value
	0	1	
Age (years)			
n	16	30	
Median (Q1, Q3)	70.5 (64.8, 74.5)	68.0 (63.3, 71.5)	0.272
Mean (SD)	71.2 (9.4)	67.8 (6.4)	
ApoE genotype, *n* (%)			
n	13	25	
ε4 carrier	2 (15)	19 (76)	0.0004
ε4 non-carrier	11 (85)	6 (24)	
Global cortical ROI			
n	16	30	
Median (Q1, Q3)	1.03 (1.01, 1.08)	1.14 (1.06, 1.27)	0.0007
Mean (SD)	1.04 (0.07)	1.18 (0.15)	
FCRST immediate free recall			
n	16	28	
Median (Q1, Q3)	15.0 (14.8, 16.0)	15.0 (13.5, 16.0)	0.756
Mean (SD)	14.6 (2.3)	13.5 (4.0)	
Clinical diagnosis, *n* (%)			
AD	2 (12)	11 (37)	
MCI	6 (38)	6 (20)	0.183
HC	8 (50)	13 (43)	

Discussion

Our results indicate that PET with florbetapir is suitable for routine use to improve the accuracy of AD diagnosis in

Table 3 SUVr values of cortical brain regions relative to the cerebellum

Region	AD (n=13)	MCI (n=12)	HC (n=21)	p-value			
				Global	AD vs. HC	MCI vs. HC	AD vs. MCI
Precuneus							
Median (Q1, Q3)	1.47 (1.24-1.60)	1.10 (0.97-1.35)	1.04 (0.98-1.06)	0.0004	<0.0001	–	0.045
Mean (SD)	1.47 (0.32)	1.19 (0.30)	1.04 (0.16)				
Anterior cingulate							
Median (Q1, Q3)	1.42 (1.25-1.56)	1.09 (1.02-1.30)	0.98 (0.92-1.09)	0.001	0.0004	0.077	0.077
Mean (SD)	1.41 (0.30)	1.18 (0.31)	1.03 (0.21)				
Posterior cingulate							
Median (Q1, Q3)	1.33 (1.14-1.46)	1.06 (0.97-1.28)	0.95 (0.82-1.02)	0.0002	<0.0001	0.030	0.030
Mean (SD)	1.33 (0.25)	1.11 (0.20)	0.96 (0.21)				
Frontal median							
Median (Q1, Q3)	1.16 (1.10-1.33)	0.97 (0.87-1.14)	0.86 (0.83-0.93)	0.0008	0.004	–	0.045
Mean (SD)	1.21 (0.22)	1.01 (0.22)	0.90 (0.17)				
Temporal							
Median (Q1, Q3)	1.37 (1.27-1.43)	1.17 (1.07-1.34)	1.12 (1.08-1.15)	0.0008	0.0001	–	0.078
Mean (SD)	1.37 (0.18)	1.20 (0.17)	1.13 (0.10)				
Parietal							
Median (Q1, Q3)	1.23 (1.16-1.28)	1.08 (0.99-1.22)	1.06 (0.99-1.10)	0.016	–	–	–
Mean (SD)	1.21 (0.17)	1.09 (0.16)	1.06 (0.13)				
Occipital							
Median (Q1, Q3)	1.14 (1.08-1.23)	1.08 (1.02-1.17)	1.06 (1.03-1.11)	0.043	–	–	–
Mean (SD)	1.17 (0.14)	1.08 (0.11)	1.07 (0.06)				
Cortex global ROI							
Median (Q1, Q3)	1.20 (1.16-1.30)	1.09 (1.02-1.24)	1.05 (1.04-1.08)	0.001	0.0001	–	0.067
Mean (SD)	1.26 (0.15)	1.12 (0.15)	1.07 (0.09)				
Hippocampus							
Median (Q1, Q3)	0.88 (0.82-0.95)	0.90 (0.82-0.96)	0.88 (0.86-0.96)	0.967	–	–	–
Mean (SD)	0.89 (0.10)	0.89 (0.09)	0.89 (0.07)				
Centrum semiovale							
Median (Q1, Q3)	1.66 (1.56-1.81)	1.61 (1.49-1.73)	1.62 (1.55-1.76)	0.743	–	–	–
Mean (SD)	1.68 (0.18)	1.63 (0.17)	1.64 (0.13)				
Posterior putamen							
Median (Q1, Q3)	1.36 (1.21-1.40)	1.23 (1.13-1.30)	1.17 (1.11-1.19)	0.005	0.004	–	–
Mean (SD)	1.31 (0.14)	1.23 (0.12)	1.16 (0.10)				
Anterior putamen							
Median (Q1, Q3)	1.44 (1.28-1.53)	1.20 (1.13-1.33)	1.14 (1.09-1.17)	0.0002	<0.0001	–	0.033
Mean (SD)	1.41 (0.17)	1.25 (0.18)	1.15 (0.14)				
Caudate nucleus							
Median (Q1, Q3)	0.83 (0.79-0.90)	0.86 (0.74-0.94)	0.90 (0.77-0.92)	0.869	–	–	–
Mean (SD)	0.85 (0.15)	0.85 (0.11)	0.86 (0.10)				
Pons							
Median (Q1, Q3)	1.49 (1.42-1.55)	1.48 (1.42-1.64)	1.52 (1.48-1.61)	0.380	–	–	–
Mean (SD)	1.49 (0.09)	1.52 (0.13)	1.54 (0.09)				

clinical settings, such as memory clinics, with acceptable tolerability and sufficient reliability. In particular, the quantitative analyses showed a higher global SUVr and SUVr in several cortical regions (precuneus, anterior and posterior cingulate, frontal median, temporal, parietal and occipital cortex) in AD patients than in HC subjects. Additionally, the SUVr in the posterior cingulate and frontal median regions was significantly higher in AD patients than in MCI

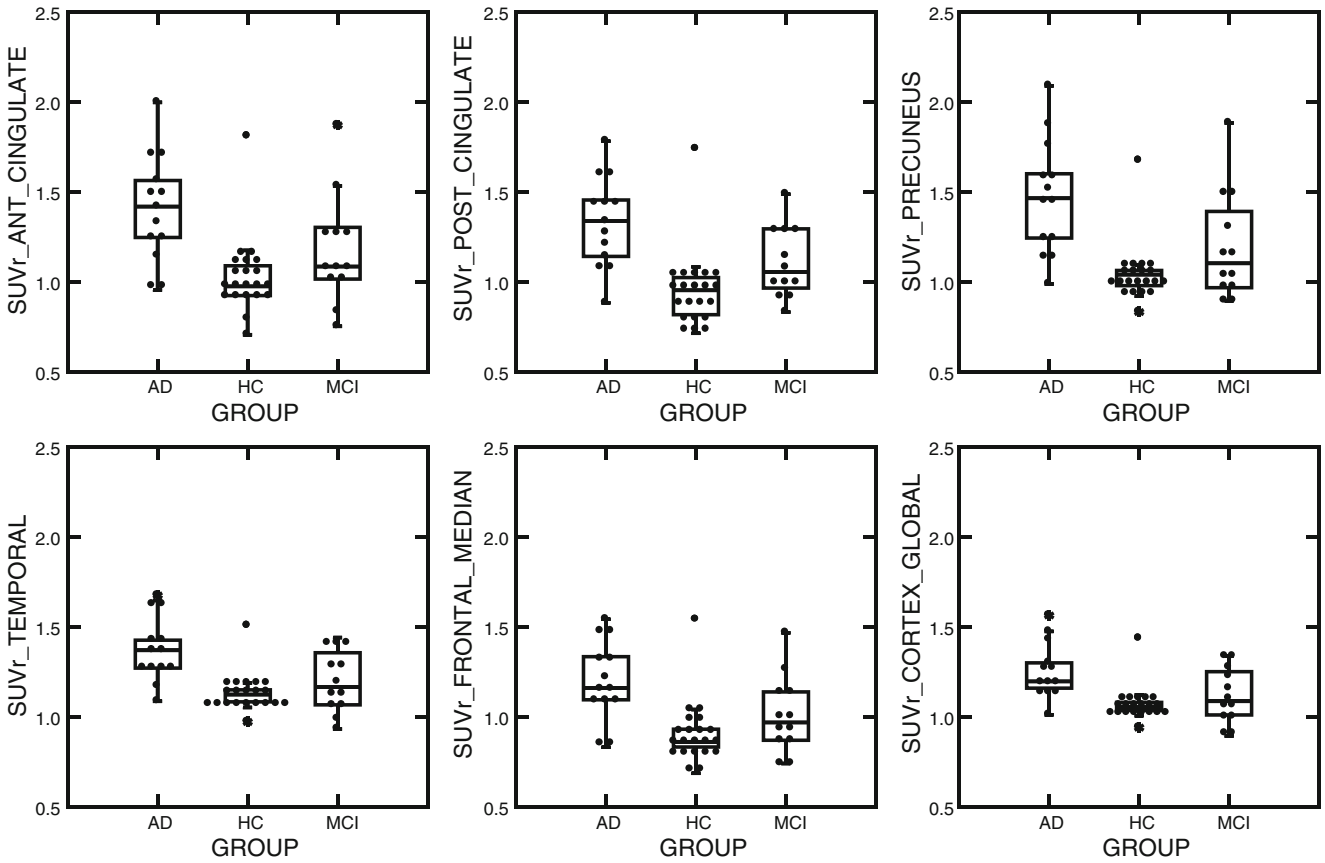

Fig. 2 SUVr values for a set of volumes of interest in AD patients, MCI patients and HC subjects

patients. To the best of our knowledge, the results of only five clinical trials with ^{18}F-labelled tracers that specifically bind to brain amyloid plaques have been published to date [15, 17, 19, 22, 25]. In all studies PET imaging with ^{18}F-labelled tracers was able to distinguish AD patients from HC subjects, but only three [15, 17, 25] included MCI patients, and the differences in SUVr between MCI patients and HC subjects were only reported with an FDDNP tracer that binds to both amyloid and tau proteins [15], which does not appear to be the case with florbetapir [25]. The pattern of florbetapir cortical uptake found in the present study is remarkably similar to that found in previous studies conducted by Wong et al. [24] and Clark et al. [22]. The pattern also appears to be similar to those found with other amyloid-labelling compounds, such as ^{11}C-PIB [10] and its ^{18}F-flutemetamol-derived molecule [17], ^{11}C -BF-227 [13], ^{18}F-FDDNP [15] and ^{18}F-BAY94-9172 [18, 19]. These patterns closely match the neuropathological stages of AD progression, which was strengthened by the high correlation found between florbetapir PET imaging and autopsy results [22]. Our results also indicate that there is high uptake of florbetapir in the white matter (centrum semiovale) and the striatum region (in particular, the putamen) to a similar degree as with other ^{11}C- [39, 40] and ^{18}F-labelled compounds [17, 41, 42]. A high rate of amyloid deposition in the striatum has been suggested to be more frequently associated with dementia with Lewy bodies [43] or some early-onset variant of AD associated with spastic paraparesis and a presenilin I (PSI) gene mutation [44]; however, this finding has also been consistently reported in PET imaging studies using amyloid ligands in AD patients [17, 39–42], and this high uptake level in the striatum does not appear to be associated with decreased glucose metabolism (as assessed by FDG PET), as it is in other cortical areas [45].

The sensitivity (92,3%) and specificity (90,5%) values provided a good quantitative assessment for the global cortex ROI, with a cut-off value (1.12) lower than that calculated by Fleisher et al. (SUVr ≥1.17), but the mean global SUVr (mean ± SD) values were also slightly lower in the present series (AD patients 1.26 ± 0.15, MCI patients 1.12 ± 0.05, HC subjects 1.07 ± 0.09) than in the study by Fleisher et al. (AD 1.39 ± 0.24, MCI 1.17 ± 0.27, HC 1.05 ± 0.16) [25]. However, the visual assessment less accurately distinguished AD patients from HC subjects, demonstrating a specificity of 38.1%. There are at least two possible explanations for this low specificity. First, the three different cameras between the three participating sites required adaptation of the reconstruction parameters to those of the tomograph with the lowest

Table 4 SUVr values in the cortical brain regions of ApoE carriers and non-carriers

Region	AD patients		MCI patients		HC subjects	
	Mean (SD)	*p*-value	Mean (SD)	*p*-value	Mean (SD)	*p*-value
Precuneus						
ε4 carrier	1.56 (0.29)	0.0167	1.37 (0.34)	0.0952	1.10 (0.24)	0.6574
ε4 non-carrier	1.09 (0.09)		0.99 (0.09)		1.00 (0.08)	
Anterior cingulate						
ε4 carrier	1.54 (0.28)	0.0167	1.38 (0.29)	0.0476	1.10 (0.30)	0.4421
ε4 non-carrier	1.03 (0.10)		0.89 (0.16)		0.97 (0.14)	
Posterior cingulate						
ε4 carrier	1.42 (0.22)	0.0167	1.27 (0.15)	0.0238	1.01 (0.32)	0.7780
ε4 non-carrier	1.02 (0.12)		0.90 (0.07)		0.92 (0.10)	
Frontal median						
ε4 carrier	1.30 (0.20)	0.0167	1.17 (0.17)	0.0238	0.98 (0.24)	0.1518
ε4 non-carrier	0.93 (0.13)		0.81 (0.11)		0.84 (0.09)	
Temporal						
ε4 carrier	1.42 (0.17)	0.0333	1.32 (0.14)	0.0952	1.15 (0.15)	0.4421
ε4 non-carrier	1.18 (0.09)		1.05 (0.10)		1.12 (0.06)	
Parietal						
ε4 carrier	1.22 (0.18)	0.6667	1.20 (0.12)	0.0476	1.08 (0.20)	0.9678
ε4 non-carrier	1.10 (0.23)		0.95 (0.09)		1.04 (0.07)	
Occipital						
ε4 carrier	1.18 (0.19)	0.6667	1.15 (0.11)	0.0952	1.08 (0.08)	0.7780
ε4 non-carrier	1.12 (0.08)		1.03 (0.09)		1.07 (0.05)	
Cortex global ROI						
ε4 carrier	1.29 (0.17)	0.1833	1.22 (0.13)	0.0952	1.09 (0.14)	0.5448
ε4 non-carrier	1.11 (0.09)		1.00 (0.09)		1.06 (0.05)	

spatial resolution (Dual Philips GEMINI) and this could have led to some borderline positive scans being rated as negative or conversely borderline negative scans being rated as positive. Second, at least one HC subject was a clear outlier, with high SUVr values and a positive visual rating. Interestingly, this HC subject had a family history of AD and was a heterozygotic ApoE4 gene carrier.

The association of the ApoE4 genotype with the likelihood of having a positive florbetapir PET scan on visual rating is another remarkable finding of this study. The association of the ApoE genotype with a higher brain amyloid load has previously been documented in several PET imaging studies with PIB [46, 47], florbetaben [19] and florbetapir [25]. Strikingly, the ApoE genotype appears to increase florbetapir uptake levels in several cortical regions in AD and MCI patients but not in HC subjects, suggesting that the presence of ApoE could strengthen or accelerate the level of amyloid deposition. Here the HC subjects with a positive scan could have been at an early preclinical stage of the disease in which criteria for MCI or AD were not yet reached, and only the follow-up will confirm its progression towards a full symptomatic feature of disease.

This study has several limitations. First, the sample size was limited, but this work was initiated and conducted in only three academic clinical settings independent of any premarketing phase II studies now being conducted by industrial sponsors. Another limitation was a possible selection bias, expressed by the significantly older age in the MCI group than in the AD and HC groups. Nevertheless, age did not differ between subjects with positive and negative scans on visual rating (Table 2). Moreover the MCI patients had a significantly older mean age than the AD patients and HC subjects. It cannot be excluded that this could have increased the mean values of florbetapir uptake in favour of showing a significant difference in relation to the HC subjects. Despite these limitations, the preliminary results indicate that imaging techniques using ^{18}F-labelled compounds, such as florbetapir, can be easily conducted in demented and predemented patients in clinical settings, such as third-level memory clinics, and could become a routine clinical procedure for patients with suspected AD. The low specificity of the visual PET scan assessment is problematic, but this could be significantly increased by improvements in the spatial resolution of tomographs as well as by the use of appropriate training programmes for raters, and by the development of semiautomatic or automatic quantifications method or software.

Conclusion

These preliminary results agree with previously reported results obtained using other PET tracers that bind to brain

amyloid plaques, and suggest that PET with florbetapir could become a routine clinical procedure to improve the reliability of AD diagnosis and the detection of typical or atypical forms of predementia stages, such as amnestic MCI and MCI associated with multidomain deficits or neuropsychiatric symptoms (e.g. depression). More studies testing the feasibility and tolerability of consecutive scans with florbetapir are needed to better document the accuracy of PET imaging with florbetapir in the AD diagnostic process at the dementia or predementia stages. Comparisons (or combinations) with other biomarkers, such as FDG PET, MRI and CSF dosages of tau and protein, are also needed. The clinical relevance of changes in quantity of brain amyloid over time, especially when disease-modifying treatments are available, should also be assessed. Finally, the reliability of visual rating of PET scans remains critical and should be urgently addressed through the improvement in spatial resolution of images, the use of semiquantitative methods and the support of appropriate training programmes for nuclear medicine physicians.

Acknowledgments This work was funded by the French Ministry of Health with grant no. PHRC-N 2008-1004 and in part by the EC-FP6-project DiMI, LSHB-CT-2005-512146, the Région Centre and FEDER: "Radex" programmes. This work was conducted with the support of the GIS Radiopharmaceutiques Caen, Toulouse, and Tours centres with Laboratoires Cyclopharma. The authors are grateful to D Skovronsky (AVID Radiopharmaceutucals), to JB Deloye (Laboratoires Cyclopharma) and to the technical staff involved in florbetapir production. Authors are also grateful to Drs. N. Daluzeau and F. Bouvier (CH Lisieux), Dr. B. Dupuy (CH Cherbourg), A. Abbas and A. Pèlerin (Inserm U923), Dr. A. Manrique (GIP Cyceron), C. Roussel, PhD, C. Baringthon, PhD, A. Matysiack, H. Bansard and F. Teasdale (CIC/CIC-IT 202) for their contributions to the clinical investigation.

References

1. American Psychiatric Association. Diagnostic and statistical manual of mental disorders. 4th ed, text revision. Washington DC: American Psychiatric Association; 2000.
2. McKhann G, Drachman D, Folstein M, Katzman R, Price D, Stadlan EM. Clinical diagnosis of Alzheimer's disease: report of the NINCDS-ADRDA Work Group under the auspices of Department of Health and Human Services Task Force on Alzheimer's Disease. Neurology. 1984;34:939–44.
3. Braak H, Braak E. Frequency of stages of Alzheimer-related lesions in different age categories. Neurobiol Aging. 1997;18:351–7.
4. Delacourte A, David JP, Sergeant N, Buee L, Wattez A, Vermersch P, et al. The biochemical pathway of neurofibrillary degeneration in aging and Alzheimer's disease. Neurology. 1999;52:1158–65.
5. Dubois B, Feldman HH, Jacova C, DeKosky ST, Barberger-Gateau P, Cummings J, et al. Research criteria for the diagnosis of Alzheimer's disease: revising the NINCDS-ADRDA criteria. Lancet Neurol. 2007;6:734–46.
6. Albert MS, DeKosky ST, Dickson D, Dubois B, Feldman HH, Fox NC, et al. The diagnosis of mild cognitive impairment due to Alzheimer's disease: recommendations from the National Institute on Aging-Alzheimer's Association workgroups on diagnostic guidelines for Alzheimer's disease. Alzheimers Dement. 2011;7:270–279
7. Klunk WE, Engler H, Nordberg A, Wang Y, Blomqvist G, Holt DP, et al. Imaging brain amyloid in Alzheimer's disease with Pittsburgh Compound-B. Ann Neurol. 2004;55:306–19.
8. Forsberg A, Engler H, Almkvist O, Blomquist G, Hagman G, Wall A, et al. PET imaging of amyloid deposition in patients with mild cognitive impairment. Neurobiol Aging. 2008;29:1456–65
9. Rinne JO, Brooks DJ, Rossor MN, Fox NC, Bullock R, Klunk WE, et al. 11C-PiB PET assessment of change in fibrillar amyloid-beta load in patients with Alzheimer's disease treated with bapineuzumab: a phase 2, double-blind, placebo-controlled, ascending-dose study. Lancet Neurol. 2010;9:363–72.
10. Mintun MA, Larossa GN, Sheline YI, Dence CS, Lee SY, Mach RH, et al. [11C]PIB in a nondemented population: potential antecedent marker of Alzheimer disease. Neurology. 2006;67:446–52.
11. Jagust WJ, Landau SM, Shaw LM, Trojanowski JQ, Koeppe RA, Reiman EM, et al. Relationships between biomarkers in aging and dementia. Neurology. 2009;73:1193–9.
12. Kudo Y, Okamura N, Furumoto S, Tashiro M, Furukawa K, Maruyama M, et al. 2-(2-[2-Dimethylaminothiazol-5-yl]ethenyl)-6-(2-[fluoro]ethoxy)benzoxazole: a novel PET agent for in vivo detection of dense amyloid plaques in Alzheimer's disease patients. J Nucl Med. 2007;48:553–61.
13. Waragai M, Okamura N, Furukawa K, Tashiro M, Furumoto S, Funaki Y, et al. Comparison study of amyloid PET and voxel-based morphometry analysis in mild cognitive impairment and Alzheimer's disease. J Neurol Sci. 2009;285:100–8.
14. Shao H, Okamura N, Sugi K, Furumoto S, Furukawa K, Tashiro M, et al. Voxel-based analysis of amyloid positron emission tomography probe [C]BF-227 uptake in mild cognitive impairment and Alzheimer's disease. Dement Geriatr Cogn Disord. 2010;30:101–11.
15. Small GW, Kepe V, Ercoli LM, Siddarth P, Bookheimer SY, Miller KJ, et al. PET of brain amyloid and tau in mild cognitive impairment. N Engl J Med. 2006;355:2652–63.
16. Thompson PW, Ye L, Morgenstern JL, Sue L, Beach TG, Judd DJ, et al. Interaction of the amyloid imaging tracer FDDNP with hallmark Alzheimer's disease pathologies. J Neurochem. 2009;109:623–30.
17. Vandenberghe R, Van Laere K, Ivanoiu A, Salmon E, Bastin C, Triau E, et al. 18F-flutemetamol amyloid imaging in Alzheimer disease and mild cognitive impairment: a phase 2 trial. Ann Neurol. 2010;68:319–29.
18. Rowe CC, Ackerman U, Browne W, Mulligan R, Pike KL, O'Keefe G, et al. Imaging of amyloid beta in Alzheimer's disease with (18)F-BAY94-9172, a novel PET tracer: proof of mechanism. Lancet Neurol. 2008;7:129–35.
19. Barthel H, Gertz HJ, Dresel S, Peters O, Bartenstein P, Buerger K, et al. Cerebral amyloid-β PET with florbetaben (18F) in patients with Alzheimer's disease and healthy controls: a multicentre phase 2 diagnostic study. Lancet Neurol. 2011;10:424–35
20. Carpenter Jr AP, Pontecorvo MJ, Hefti FF, Skovronsky DM. The use of the exploratory IND in the evaluation and development of 18F-PET radiopharmaceuticals for amyloid imaging in the brain: a review of one company's experience. Q J Nucl Med Mol Imaging. 2009;53:387–93.
21. Choi SR, Golding G, Zhuang Z, Zhang W, Lim N, Hefti F, et al. Preclinical properties of 18F-AV-45: a PET agent for Abeta plaques in the brain. J Nucl Med. 2009;50:1887–94.

22. Clark CM, Schneider JA, Bedell BJ, Beach TG, Bilker WB, Mintun MA, et al. Use of florbetapir-PET for imaging beta-amyloid pathology. JAMA. 2011;305:275–83.
23. Lin KJ, Hsu WC, Hsiao IT, Wey SP, Jin LW, Skovronsky D, et al. Whole-body biodistribution and brain PET imaging with [18F]AV-45, a novel amyloid imaging agent – a pilot study. Nucl Med Biol. 2010;37:497–508.
24. Wong DF, Rosenberg PB, Zhou Y, Kumar A, Raymont V, Ravert HT, et al. In vivo imaging of amyloid deposition in Alzheimer disease using the radioligand 18F-AV-45 (flobetapir F 18). J Nucl Med. 2010;51:913–20.
25. Fleisher AS, Chen K, Liu X, Roontiva A, Thiyyagura P, Ayutyanont N, et al. Using positron emission tomography and florbetapir F18 to image cortical amyloid in patients with mild cognitive impairment or dementia due to Alzheimer disease. Arch Neurol. 2011;68:1404–11
26. Petersen RC, Smith GE, Waring SC, Ivnik RJ, Tangalos EG, Kokmen E. Mild cognitive impairment: clinical characterization and outcome. Arch Neurol. 1999;56:303–8.
27. Sarazin M, Berr C, De Rotrou J, Fabrigoule C, Pasquier F, Legrain S, et al. Amnestic syndrome of the medial temporal type identifies prodromal AD: a longitudinal study. Neurology. 2007;69:1859–67.
28. Mattis S. Mental status examination for organic mental syndrome in the elderly patient. In: Bellak L, Karasu TB, editors. Geriatric psychiatry. New York: Grune & Stratton; 1976. p. 77–121.
29. Grober E, Buschke H, Crystal H, Bang S, Dresner R. Screening for dementia by memory testing. Neurology. 1988;38:900–3.
30. Deloche G, Hannequin D, Dordain M, Perrier D, Pichard B, Quint S, et al. Picture confrontation oral naming: performance differences between aphasics and normals. Brain Lang. 1996;53:105–20.
31. Golden CJ, Hammeke TA, Purisch AD. Diagnostic validity of a standardized neuropsychological battery derived from Luria's neuropsychological tests. J Consult Clin Psychol. 1978;46:1258–65.
32. Mahieux-Laurent F, Fabre C, Galbrun E, Dubrulle A, Moroni C. Validation of a brief screening scale evaluating praxic abilities for use in memory clinics. Evaluation in 419 controls, 127 mild cognitive impairment and 320 demented patients. Rev Neurol (Paris). 2009;165:560–7.
33. Rey A. Manuel: test de copie et de reproduction de mémoire de figures géométriques complexes. Paris: Centre de Psychologie Appliquée; 1959
34. Jensen AR. Scoring the Stroop test. Acta Psychol. 1965;24:398–408.
35. Wechsler D. Wechsler Memory Scale Revised manual. San Antonio: The Psychological Corporation; 1987
36. Reitan R. Validity of the Trail Making Test as an indicator of organic brain damage. Percept Mot Ski. 1958;8:271–6.
37. Liu Y, Zhu L, Plössl K, Choi SR, Qiao H, Sun X, et al. Optimization of automated radiosynthesis of [18F]AV-45: a new PET imaging agent for Alzheimer's disease. Nucl Med Biol. 2010;37:917–25
38. R Development Core Team. R: A language and environment for statistical computing. R Foundation for Statistical Computing, Vienna, Austria; 2011. ISBN 3-900051-07-0. URL http://www.R-project.org
39. Ikonomovic MD, Klunk WE, Abrahamson EE, Mathis CA, Price JC, Tsopelas ND, et al. Post-mortem correlates of in vivo PiB-PET amyloid imaging in a typical case of Alzheimer's disease. Brain. 2008;131:1630–45.
40. Raji CA, Becker JT, Tsopelas ND, Price JC, Mathis CA, Saxton JA, et al. Characterizing regional correlation, laterality and symmetry of amyloid deposition in mild cognitive impairment and Alzheimer's disease with Pittsburgh Compound B. J Neurosci Methods. 2008;172:277–82.
41. Rowe CC, Ng S, Ackermann U, Gong SJ, Pike K, Savage G, et al. Imaging beta-amyloid burden in aging and dementia. Neurology. 2007;68:1718–25.
42. Villemagne VL, Ong K, Mulligan RS, Holl G, Pejoska S, Jones G, et al. Amyloid imaging with (18)F-florbetaben in Alzheimer disease and other dementias. J Nucl Med. 2011;52:1210–7.
43. Halliday G, Song Y, Harding A. Striatal β-amyloid in dementia with Lewy bodies but not Parkinson's disease. J Neural Transm. 2011;118:713–9.
44. Koivunen J, Verkkoniemi A, Aalto S, Paetau A, Ahonen JP, Viitanen M, et al. PET amyloid ligand [11C]PIB uptake shows predominantly striatal increase in variant Alzheimer's disease. Brain. 2008;131:1845–53.
45. Furukawa K, Okamura N, Tashiro M, Waragai M, Furumoto S, Iwata R, et al. Amyloid PET in mild cognitive impairment and Alzheimer's disease with BF-227: comparison to FDG-PET. J Neurol. 2010;257:721–7.
46. Reiman EM, Chen K, Liu X, Bandy D, Yu M, Lee W, et al. Fibrillar amyloid-beta burden in cognitively normal people at 3 levels of genetic risk for Alzheimer's disease. Proc Natl Acad Sci U S A. 2009;106:6820–5.
47. Grimmer T, Tholen S, Yousefi BH, Alexopoulos P, Forschler A, Forstl H, et al. Progression of cerebral amyloid load is associated with the apolipoprotein E epsilon4 genotype in Alzheimer's disease. Biol Psychiatry. 2010;68:879–84.